International Journal of
Plasma Environmental Science and Technology

Regular Paper

DOI: 10.34343/ijpest.2024.18.e01004

Plasma candle with a hollow dielectric cylinder for a wide and stable jet

Ayman A. Abdelaziz[1, 2,*], Nozomi Takeuchi[3], Yoshiyuki Teramoto[1], and Hyun-Ha Kim[1,*]

[1] National Institute of Advanced Industrial Science and Technology (AIST),
Environmental Management Research Institute, 16-1 Onogawa, Tsukuba, Ibaraki 305-8569, Japan
[2] Faculty of Science, Assiut University, Assiut 71516, Egypt
[3] Department of Electrical and Electronic Engineering, Tokyo Institute of Technology,
2-12-1 Ookayama, Tokyo 152-8552, Japan

* Corresponding author: ayman.kotb@aist.go.jp (Ayman A. Abdelaziz), hyun-ha.kim@aist.go.jp (Hyun-Ha Kim)

Received: 2 February 2024
Revised: 4 April 2024
Accepted: 18 April 2024
Published online: 20 April 2024

Abstract

Expanding a nonthermal plasma jet to treat a large area is considered as one of the big challenges for industrial applications. Unlike conventional upscaling methods using multi-tubes, this work reports a new approach to obtain a stable, large-volume, wide-area, and long plasma plume from a single tube. The wide plasma jet is achieved using a hollow dielectric cylinder (HDC) embedded perpendicular to the flow of helium inside a wide glass tube (diameter: 26 mm). In addition to the capability of the developed device to launch long and wide plasma plumes, it exhibits low operating power that makes the plasma plume maintain at a temperature close to the room temperature. Furthermore, the jet has a flickering pattern resembling a candle flame, similar to the observed phenomenon in the recently developed plasma candle device utilizing a microporous disc. Additionally, the millimeter-sized hollows in the HDC prevent any pressure drop across it, offering a distinct advantage over plasma candle devices. The investigation revealed that the narrow channels within the HDC intensify the electric field in the device, which is necessary to overcome the comparatively weak electric field in the wide tube. To gain deeper insights into the pivotal factors contributing to launching a stable plasma jet, the plume was monitored using a high-speed camera under different configurations of the developed device. It is found that the arrangement of the HDC locations and the electrodes inside the glass tube are important to form a stable plasma jet; two distinct plasma zones are observed inside the developed device and optimizing their ratio is a crucial parameter contributing to launching a strong, stable, and wide plasma jet. The presented techniques and findings can be applied to improve the uniformity of plasma jets launched from conventional multi-tube devices.

Keywords: Plasma candle, jet diameter expansion, hollow dielectric cylinder (HDC), narrow gas channels, single tube.

1. Introduction

Considerable attention has been paid to nonthermal plasma for various manufacturing processes following its successful application for ozone synthesis [1, 2]. Conventionally, the generated plasma was confined between two electrodes with varying designs, posing challenges in uniformity treating materials that couldn't be inserted between electrodes or were thermally sensitive. In the early 1990s, significant progress was achieved by developing a technique to extend the plasma away from the reactor, and different names were assigned to this extended plasma, such as nonthermal atmospheric pressure plasma jet (N-APPJ), cold atmospheric pressure plasma jet, and nonequilibrium plasma jet [3−5]. However, these early jets were characterized by being short, lacking uniformity and stability, and requiring higher flow rates of inert gases. Consequently, optimizing operating conditions and devices configurations to launch a plasma jet with satisfactory properties became a hot topic and a subject of intensive studies for material and surface processing applications. In 2005, Lu and Laroussi made a substantial modification in the N-APPJ source, enabling the formation of a long plasma jet launched from a narrow tube at lower flow rates and electrical power, with a temperature close to the atmospheric levels [6, 7]. This progress extended the applications of the plasma jet to include biology and biomedical applications [8−10]. Typically, a plasma jet or plume is formed through the electrical excitation of

gases that have long lifetime excited species (mostly inert gas, such as He, Ar or Ne) flowing inside a narrow tube. As a result, the gas discharge extends from the nozzle of the tube, reacting with surrounding air and delivering chemically reactive media to a target material [11, 12]. This enables the separation of the material undergoing plasma treatment from the plasma generation zone. During the last two decades, various N-APPJ devices and techniques have been developed and investigated for different applications [13−18].

Nevertheless, a critical challenge for industrial applications remains the scaling up of the plasma jet device to effectively expand the treatment area. Hence, considerable attempts have been implemented to develop controllable and scalable plasma jet devices. Traditional approaches of using bundle arrays of multi-tubes in one and two dimensions have been proposed as potential solutions [19, 20]. However, challenges arise with these methods, as the multi-jets generated fail to uniformly treat the intended targets. The hydrodynamic (induced by gas flow and heating) and electrical interactions (induced by the Coulomb repellence force) occur among the jets in the array are highly sensitive to the operating conditions, electrode structure, and tube spacing [21−23]. These interactions lead to divergence in the outer plumes and negatively affect the treatment uniformity. Therefore, generating a wide atmospheric pressure plasma jet using a single tube is of great interest. In the last decade, a few attempts have been made to increase the tube diameter to 10–16 mm in plasma jet devices [24, 25]; however, their practical applications are limited either due to the inhomogeneities of the launched jet [25] or the operating restrictions in obtaining a stable jet [24]. The problems of obtaining a stable jet from a wide single tube have remained largely unknown until our thorough investigation aimed at elucidating the primary barriers to attaining a uniform, stable, and long plasma jet from such a configuration [26, 27]. The comprehensive study emphasized the crucial role of controlling flow dynamics and intensifying the electric field within the wide tube of the plasma jet device. An inherent challenge arises due to the sudden expansion of the gas within the wide tube, inducing turbulent gas flow for long distances, reaching the nozzle in the typical device lengths. This turbulent flow not only hinders the jet formation but also impedes the discharge ignition. Moreover, the investigation revealed that an increase in the tube diameter leads to a significant reduction in the electric field, negatively affecting the discharge properties. To address these challenges, we introduced a novel type of plasma jet device capable of generating a uniform and stable plasma jet with a diameter of 20 mm [28]. This device is named a “plasma candle” due to its resemblance to a flickering candle flame [29, 30]. The incorporation of a microporous ceramic disc in this device plays a pivotal role in generating a uniform and stable plasma jet due to its role in modifying flow dynamics and discharge characteristics.

In this study, another device capable of generating a long and stable atmospheric pressure plasma jet with a diameter of 26 mm is presented, a result that would be difficult to obtain using conventional configurations of plasma jet sources. This achievement was realized by incorporating a hollow dielectric cylinder (HDC) with millimeter-sized perforations into a wide tube (inner diameter: 26 mm).

2. Experimental details and electric field calculation

The schematic diagram and photograph of the developed device are shown in Fig. 1. The plasma source is made of two glass tubes (inlet and outlet tubes), and a ceramic HDC is fixed between the two tubes, as shown in Fig. 1 (a). The inner diameter of each glass tube is 26 mm, and the outer diameter is 30 mm. Various lengths of the inlet and outlet tubes are used in the present study. The length and diameter of the HDC are 44 and 26 mm, respectively. Unlike the microporous disc in the plasma candle device, the hollow spaces in the HDC-based device have diameters ranging from 1 to 2 mm, serving as narrow gas channels. As a result, almost no pressure-drop across the HDC compared to the recently developed plasma candle device that uses microporous disc, as illustrated in Fig. 1 (b). The cross-section of each channel in the present device resembles the shape of a waterdrop, with its rounded contours and tapering edges, and they are arranged as illustrated in Fig.1 (c). He (99.995% purity) was used as the operating gas, and its flow rate (Q) was controlled using a mass flow controller. To prevent gas leakages, the junctions between the HDC and the glass tubes were precisely sealed using Teflon tape and silicone adhesion. Two thin copper tapes, used as high-voltage (HV) and ground electrodes, are fixed in various locations around the outer surface of the outlet glass tube and the HDC. The gas temperature of the plasma jet was measured using a fiber optic thermometer (Anritsu, Amoth FX8500, with a temperature resolution of 0.1 °C), and its dielectric tip was placed 5 mm from the tube nozzle inside the plasma plume, as shown in Fig. 1 (a).

To ignite a discharge, an AC power supply (Tamaoki Electronics Co., TE-HFV1520K-0400) with a peak-to-peak voltage (V_{pp}) of up to 19 kV and a frequency of 15 kHz was used to deliver high voltage to the HV electrode. The applied voltage and the associated current were measured using a high voltage probe (Tektronix P6015A) and a current monitor (Pearson current transformer Model 2877), respectively, and their signals were monitored using an oscilloscope (Tektronix DBP 2024B). Given helium's characteristic of having a lower breakdown voltage compared to air, the discharge manifested inside the tube without any observable flashover outside across the applied voltage range. This has been confirmed by monitoring the current behavior when helium was not flowing through the tube. The consumed power was determined using the Lissajous diagram based-technique [31].

Photographs of the plasma jet were captured using a digital single-lens reflex (DSLR) camera (Cannon EOS 60D) with an exposure time of 166 ms and ISO of 1000. The dynamic behavior of the plume was observed using the Schlieren imaging technique, facilitated by a high-speed camera (Photron, FASTCAM SA1.1) set at a frame rate of 15000 fps and an exposure time of 20.54 µs. For this purpose, the high-speed camera, the jet device, and two spherical mirrors with a diameter of 110 mm and a focal length of approximately 1 m were arranged in a Z-type system.

To determine the role of the HDC on the ignition of the plasma in the developed device, the electrostatic field in the tube with and without the HDC was calculated when the plasma was off. The electric field strength and its distribution were calculated using COMSOL Multiphysics modeling software (Ver. 5.4) at a constant applied voltage (15 kV), where the relative permittivity of the ceramic and glass were assumed to be 8.5 and 3.8, respectively.

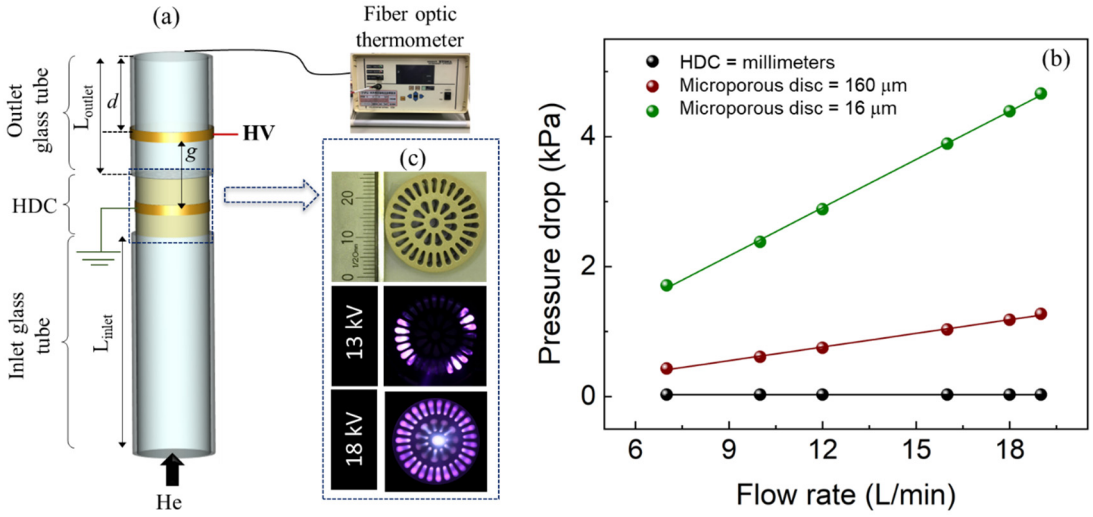

Fig. 1. (a) Schematic of the developed plasma jet source. (b) relationship between the pressure drop and flow rate for the HDC and conventional plasma candle device that uses a microporous disc with various pore sizes (160 and 16 µm) and a diameter of 26 mm. (c) Photographs show the cross-section of the HDC and top views of the device at various voltages and Q = 18.7 L min^{-1}.

3. Results and discussion

3.1. Jet formation and its properties

Fig. 2 depicts the effect of the HDC on plasma jet formation. Using a wide glass tube (diameter: 26 mm) without an HDC, the jet only started to appear at high flow rates (Q > 18 L min^{-1}). However, the plume was nonuniform (stochastic and nonsymmetric) and unstable, as shown in Fig. 2 (a). Increasing the applied voltage adversely affected the jet formation, where the jet extinguished (Fig. 2 (b)). These difficulties in forming a stable plasma jet are attributed to intense turbulence at the tube nozzle [27], facilitating the entertainment of the surrounding air inside the tube. Consequently, the He ratio inside the tube is reduced, hindering the ignition of the discharge. The higher flow rate expels the air facilitating the discharge ignition, but the high turbulence

outside the tube makes the jet flicker randomly [26, 27]. Furthermore, increasing the applied voltage induces more electrohydrodynamic force and increases the entrainment of the surrounding air.

On the other hand, Fig. 2 (d) shows that a stable jet was launched when an HDC was inserted inside the glass tube (Fig. 2 (d)). This jet was launched in conical shape (similar to that observed in the conventional narrow plasma jet devices) with a length of 50 mm and was sustained at flow rates much lower than those observed without the HDC. The jet exhibits a flickering resemblance to a candle flame, similar to the observed phenomenon in the plasma candle device employing a microporous disc. Furthermore, it is observed that the ignition voltage reduced from 18 to 10 kV, and the sustained voltage decreased from 14 to 8 kV when the HDC was used. This phenomenon of igniting the discharge at a much lower voltage when the HDC inserted inside a wide glass tube is attributed to the significant effect of the HDC on the flow dynamic and the discharge characteristics. Fig. 3 shows the laminar flow of the gas as it exits the tube over a considerable distance in the developed device, resulting in the formation of a conical-shaped jet. Additionally, the presence of the HDC significantly intensified the electric field, as shown in Fig. 4. This intensification in the electric field strength is not achievable in the tube without the HDC, even by reducing the gap between the electrodes (Figs. 4 (a) −(c)). This increase in the electric field strength significantly affects the plasma characteristics, including a decrease in the breakdown voltages, an increase in the average electron density, density of generated species, and the velocity of the ionization wave [32−36]. Consequently, a stronger, stable, and more uniform wide plasma jet was obtained when the HDC was used. However, the properties of the HDC (such as the dielectric constant, hole sizes, and length) might significantly affect the electric field, as shown in Figs. 4 (d) and (e), where the electric field reduced when glass was assumed to be the HDC material instead of ceramic. Furthermore, Fig. 4 shows that the electric field at the contour gas channels of the HDC is slightly higher than those located at the center of the HDC. Therefore, the discharge appeared inside the contour gas channels of the HDC at lower applied voltages, while it needs much higher voltages to appear in all holes, as shown in Fig. 1 (c).

The effect of the HDC on the electrical properties of the developed device is also evidenced from the current waveform, as shown in Fig. 5. The applied voltage has a step shape; therefore, the capacitive current was characterized by two current peaks per half-cycle of the applied voltage. Meanwhile, the discharge current features a single peak per half-cycle, with its activities vanishing at the peak and zero values of the applied voltage (owing to $dV/dt = 0$). Fig. 5(a) shows a remarkable increase in the discharge current when using the HDC, despite its effect on the capacitive current being minor (Fig. 5 (b)). This indicates that the HDC in this configuration boosts the discharge with no significant effects on the capacitance of the device. The power consumed in this configuration of the developed device was about 20 W, and the associated increase in the jet temperature (ΔT) measured 3 min after the operation at the nozzle of the glass tube was only about 17 °C. The low operating power and the low jet temperature make this jet source suitable to treat temperature-sensitive materials, including the human body. It is worth noting that there were no noticeable changes in the jet properties when a shorter HDC (about 22 mm) was used.

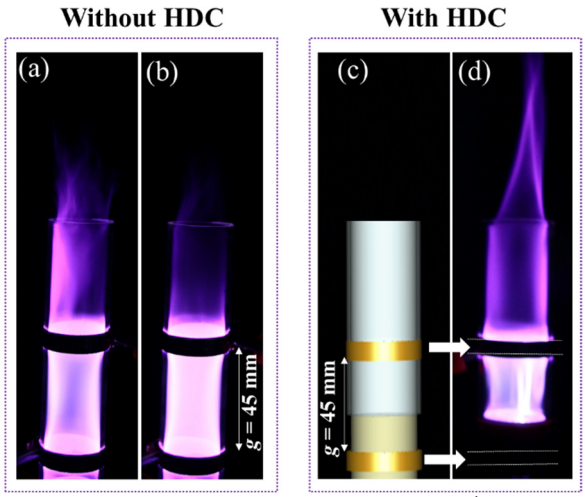

Fig. 2. Influence of the HDC on jet formation at Q = 18.7 L min^{-1}; (a) glass tube without HDC at V_{pp} = 16.0 kV; (b) glass tube without HDC at V_{pp} = 19.0 kV. (c) Schematic of the device configuration with HDC, and (d) glass tube with HDC at V_{pp} = 16.0 kV.

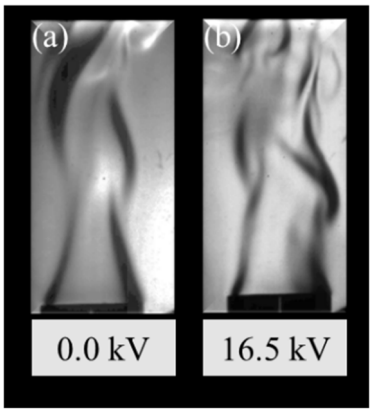

Fig. 3. Schlieren images of the gas flow from the HDC at Q = 18.7 L min^{-1}: (a) V_{pp}= 0.0 kV and (b) V_{pp}=16.5 kV.

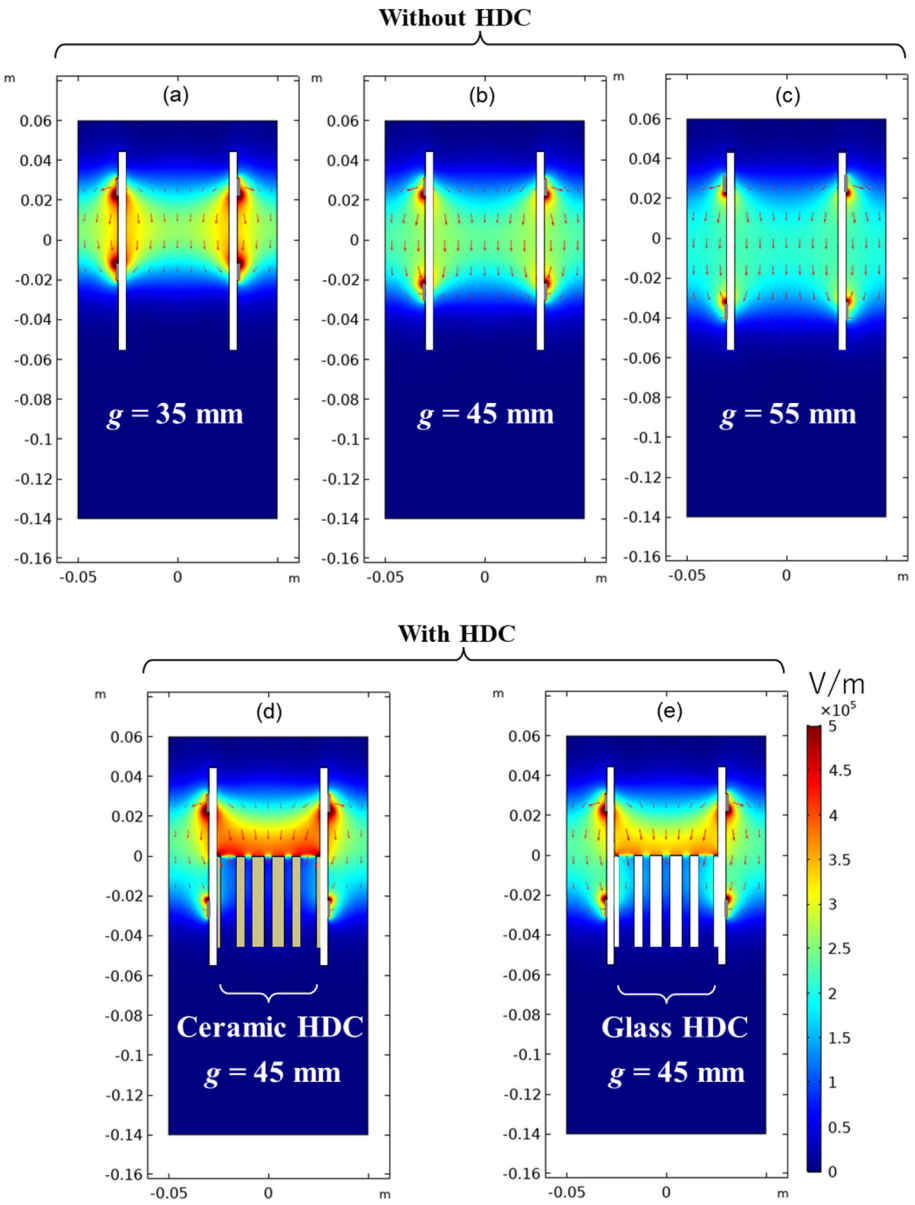

Fig. 4. Electric field strength and its distribution in a glass tube (a-c) without the HDC at different discharge gaps and (d-e) using HDC with different materials at the same applied voltage.

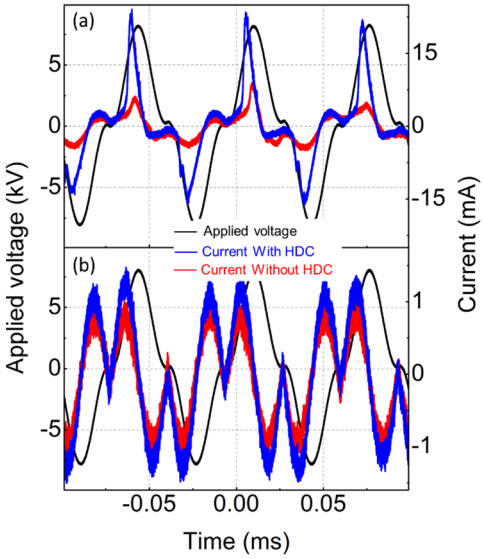

Fig. 5. Current-voltage waveforms for the tube with and without HDC at the same applied voltage (V_{pp} = 16 kV) and discharge gap (g = 45 mm); (a) total current and (b) capacitive current (i.e., a condition without helium and, consequently, the absence of discharge).

3.2 Design Considerations for Improved Jet Properties

To gain insight into the performance of the developed HDC device aimed at achieving a stable jet formation, the discharge and jet properties across various configurations are systematically examined. This included variations in the lengths of input and outlet tubes, as well as different electrode arrangements. This comprehensive analysis allows us to understand the distinct roles of each component, facilitating the optimization of the device configuration for practical applications.

3.2.1 The role of inlet and outlet tubes

To understand the role of the inlet and outlet tubes and optimize their lengths, the jet formation without and with tubes at various lengths is investigated. Fig. 6 shows the jet formation when the outlet tube disconnected, while the HDC remains fixed and tightly sealed with the inlet tube. In this configuration, the HV and ground electrodes were wrapped around the HDC and inlet tube, respectively. It is notable that the discharge first appeared in the region between the HDC and the ground electrode at a relatively low applied voltage (~ 5 kV), following which the discharge appeared in the gas channels of the HDC, and this in turn was followed by the jet formation. Visually, the jet properties (including its length, diameter, and brightness) are adversely affected by decreasing the flow rate. The largest jet (diameter: ~ 16 mm; length: ~ 57 mm) was achieved at a flow rate of 18.7 L min^{-1}, and it decreased linearly in size with the reduction in the flow rate to 11.6 L min^{-1}. A further decrease in the flow rate to 10 L min^{-1}caused a drastic reduction in the plasma properties (Fig. 6 (h)), and jet formation ceased at lower flow rates (< 10 L min^{-1}). To explain the confinement of the plasma jet within a diameter of only 16 mm at the center of the HDC despite the ignition of the plasma at the contour holes of the HDC, the flow dynamic is monitored using Schlieren technique, as shown in Fig. 7. As can be seen, He exits the holes of the HDC in the form of separated narrow multi-plumes, subsequently merging after a short distance from the HDC. This pattern increases the exposed area of the plume to the surrounding air, allowing it to infiltrate and mix with the helium exiting from the contour holes. On the other hand, the helium exiting from the central wide holes is shielded by that which exits from the contour holes. At lower flow rates, the ambient air has higher ability to entrain the jet and mix with the He, leading to a reduction in the helium mole fraction, which plays a key role in jet formation [37].

To reduce the adverse effect of mixing the surrounding air with He, a glass tube (the outlet glass tube in Fig. 1 (a)) was attached to the HDC [38]. As can be seen in Fig. 8, the presence of the outlet tube has a significant effect on the jet formation and its properties. Additionally, the longer outlet tube mitigates the turbulence, which is another important role in jet formation [26]. Increasing the outlet tube length to 80 mm leads to an increase in the jet length as well as its diameter to 75 mm and 26 mm, respectively. However, the

jet intensity weakens with an increase in the length of the outlet glass tube, and the jet is extinguished when the length of the outlet tube equals 90 mm. This phenomenon is attributed to the quenching of the He excited species and the loss of charges inside the longer outlet tube, which resulted from the lowered the ionization coefficient (α) in this region.

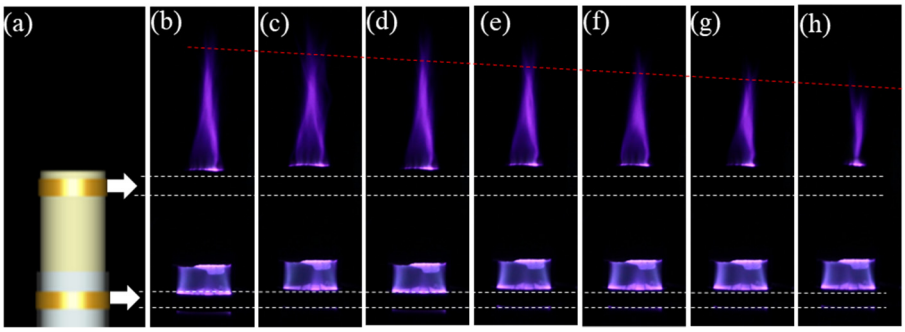

Fig. 6. (a) schematic of the device configuration. (b-h) Influence of the HDC on jet formation when g = 45 mm, V_{pp} = 13 kV and flow rates of (b) Q = 18.7 L min^{-1}, (c) Q = 17.3 L min^{-1}, (d) Q = 15.8 L min^{-1}, (e) Q = 14.4 L min^{-1}, (f) Q = 13 L min^{-1}, (g) Q = 11.6 L min^{-1}, and (h) Q = 10 L min^{-1}. The red dashed line shows the gradual decrease in the jet length with the decrease in the flow rates, while the white dashed lines show the locations of the HV and ground electrodes.

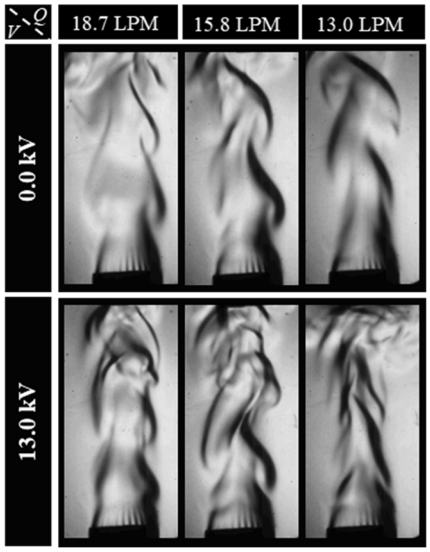

Fig. 7. Schlieren images of the gas flow from the HDC at different flow rates without discharge and at V_{pp} = 13 kV.

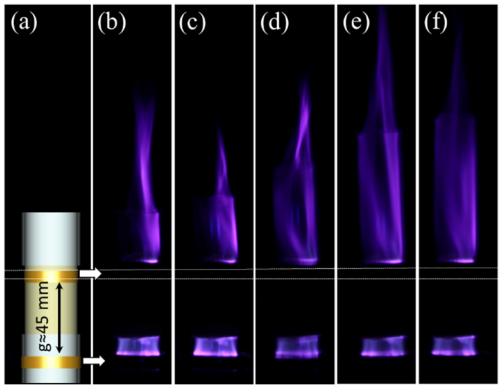

Fig. 8. (a) Schematic of the device configuration. (b-f) Photographs of the jet at Q = 18.7 L min^{-1}, V_{pp} = 13 kV, for different lengths of the outlet tube; (b) 20 mm, (c) 30 mm, (d) 40 mm, (e) 60 mm, (f) and 80 mm.

In addition to the importance of the outlet tube length, the input tube length emerges as another critical factor influencing the functionality of this device. As depicted in Fig. 9, using a short tube of 30 mm length before the HDC resulted in launching a thin and short jet. This is attributed to the high flow rate of the inlet gas, which has insufficient distance for diffusion and distribution to the HDC channels [27, 30]. Consequently, the gas primarily enters from the center hole of the HDC, corresponding to the main gas inlet, and this strong gas flow passes through without substantial diffusion in the outlet tube, as illustrated in Fig. 9 (b) and (c). The ratio of L/D (where L is the tube length and D is its diameter) plays a crucial role in controlling the flow dynamics within the device, as described in detail in prior works [27, 30]. Thus, to address this challenge, extending the length of the inlet tube to at least 8 mm in this configuration proves effective. This flow dynamics pattern was not observed when employing a microporous disc in the plasma candle device. In that configuration, the plume exhibited a laminar and stable flow, covering the entire diameter of the tube, even with a very short distance before the disc [29, 30]. Therefore, the size of the holes in the disc is critical, indicating that the length of the device could be considerably reduced by tuning the size of hollows in the HDC. Alternatively, a more practical approach could involve the use of a gas diffuser at the short tube before the HDC. This method ensures uniform gas distribution into the HDC channels, as we proposed in a previous work [27].

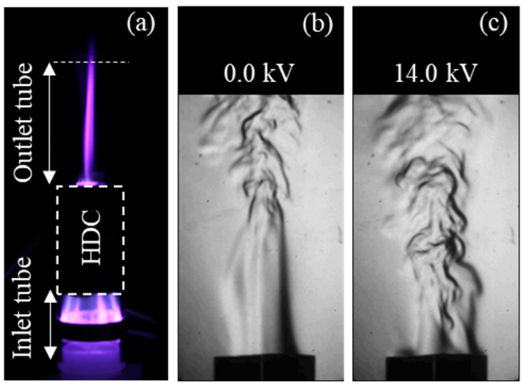

Fig. 9. (a) A photograph of the discharge and resultant jet in the device under conditions of Q = 18.7 L min^{-1}, V_{pp} = 14.0 kV, with inlet and outlet tube lengths of 30 mm and 60 mm, respectively. (b) and (c) Schlieren images of the gas flow in the device at V_{pp} = 0.0 and 14.0 kV, respectively, maintaining the configuration described in (a). The dashed rectangular and horizontal lines in (a) show the location of the HDC and the nozzle of the outlet tube, respectively.

3.2.2 The influence of the electrode locations

It is observed that increasing the applied voltage in the previous configuration did not result in a noticeable change in the jet morphology but led to a strong backward discharge in the inlet tube. Alternatively, we proposed a modification in the positions of the ground and HV electrodes, wrapping them around the HDC and the outlet glass tube, respectively, as shown in Fig. 10. As can be seen, a remarkable effect of the position of the HV electrode on the jet formation. At shorter HV electrode distances (around 20 mm) from the HDC, a strong discharge appeared in the electrode gap (between the HV electrode and the HDC), and filaments were observed along with the glow discharge. The number of discharge filaments decreased as the distance between the HV electrode and the HDC increased (≥ 30 mm), and eventually a clear glow discharge with almost no filaments ware observed at a larger gap and the same applied voltage. Notably, distinct plasma regions were observed in the device, as follows: The first plasma region was noticed in the gas channels of the HDC and the space between the HV electrode and the HDC inside the tube. The second plasma region was observed between the HV electrode and the nozzle of the outlet tube, as shown in Fig. 10. Similar to the electrostatic field calculation depicted in Fig. 4, it is expected that the highest electric field occurs between the electrodes and weakens beyond the HV electrode in the direction of the tube nozzle during the discharge. Fig. 10 also indicates the importance of tunning the ratio between these regions to obtaining a uniform and strong emission jet. At small gaps between the electrodes (i.e., at around 20 mm gap between the HV electrode and the HDC), only a dim plasma jet can be obtained. This phenomenon differs from the plasma candle device using a microporous disc, where a jet with strong emission was achieved even at very short distances (a few millimeters) between the HV electrode and the microporous disc. This difference is more likely attributed to the stronger effect of the microporous disc on the electric field and pressure drop. Hence, the optimization of the electrodes and

HDC arrangements is crucial in the present device, as the observed discharge regions play pivotal roles in controlling the amount of generating and losing species, influencing the overall flow dynamics. The jet became stronger when the first region increased, and it associated with a decrease in the threshold power to launch a jet from 20 W to 10 W when the *d* decreased from 55 to 22 mm. The improvement of the jet properties is attributed to the expanded electrode gap, which increased the discharge volume and residence time of the species, even at the low electric fields. However, at a much larger gap (i.e., when $d \leq 22$ mm), the high amount of the generated species induces stronger perturbation, which cannot be recovered at the short distance to the tube nozzle. Consequently, the jet length was detracted. The optimum distance *d* in the present study was about 40−48 mm. This study suggests that enhancing the traditional scaling approach of a bundle of narrow tubes for jet formation can be achieved by incorporating an outlet tube to the nozzle of the narrow tubes and strategically rearranging the electrode locations.

In addition to the effect of the electrode arrangement on the jet properties, their width plays another important role. Increasing the width of the ground electrode (W_g) to 16 mm enhances jet formation in terms of reducing the initiation voltage and increasing the jet intensity (Fig. 11), similar to that observed in conventional plasma jets [39]. The wider ground electrode could lead to a jet formation even at low flow rates (7.2 L min^{-1}), which was difficult to achieve when the width of the ground electrode was 8 mm. This finding could indicate that the area of intensified electric field inside the HDC increases, and the equivalent reactance of the plasma jet decreases as the width of the ground electrode increases. Furthermore, the HV electrode width (W_{HV}) was found to have an effect similar to that of the ground electrode width.

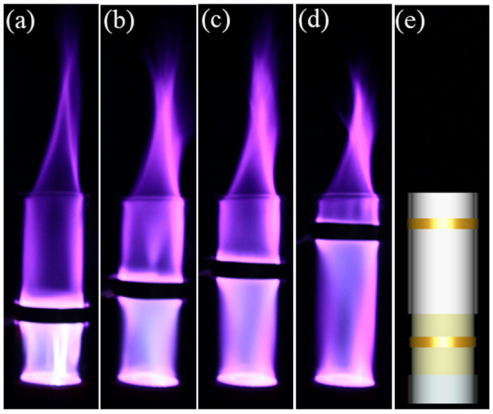

Fig. 10. (a−d) Photographs of the launched jet from the device at Q = 18.7 L min^{-1}, V_{pp} = 16 kV, L_{outlet} = 80 mm, and different *d*s *(a)* 55 mm, (b) 45 mm, (c) 35 mm, and (d) 22 mm. (e) Schematic diagram of the device configuration for (d).

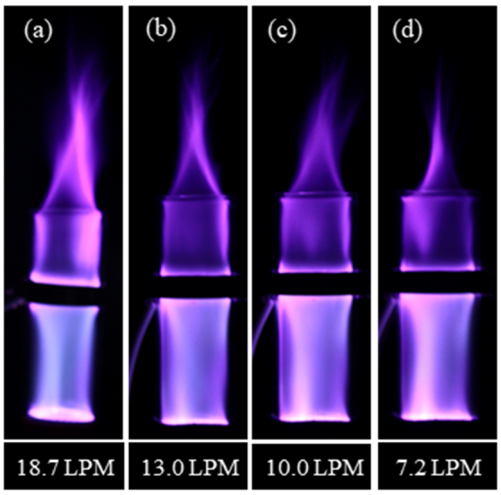

Fig. 11. Photographs of jet launched from the developed device at W_g = 8 mm, W_{HV} = 8 mm, V_{pp} = 16 kV, and different flow rates.

4. Conclusion

A new plasma source was developed to launch a wide plasma jet at atmospheric pressure from a single tube with high stability for material surface and biomedical treatments. The new device involves a hollow dielectric disc (HDC) with millimeter-sized hollows into a wide tube with a diameter of 26 mm. The intensification of the electric field and the modifications of the flow dynamics by the HDC played key roles in the discharge initiation and the jet formation. The discharge inside the gas channels of the HDC played a key role in the jet formation. The launched jet exhibits properties similar to the observed phenomenon in the plasma candle device employing a microporous disc, while the HDC-based device demonstrates the advantage of no pressure drop. Furthermore, the experimental results demonstrated that the length and intensity of the plasma jet can be increased significantly using an appropriate combination of the tube length and the electrodes position with respect to the HDC. These arrangements play a crucial role in the plasma volume and field distribution, which significantly affect the jet properties. Therefore, optimization of these parameters is important for effectively and practically launching a wide plasma jet at a lower flow rate and power. Finally, we believe that the outstanding features of the newly invented plasma jet with an HDC is promising for existing plasma jet applications and can open gateways to new applications for plasma jets. Furthermore, its concept can be used to improve the efficiency of the current plasma jet devices launched from small tubes.

References

[1] Kim H.-H., Abdelaziz A. A., Teramoto Y., Nozaki T., Kim D.-Y., Brandenburg R., Schiorlin M., Hensel K., Song Y.-H., Lee D.-H., Kang W. S., and Mizuno A., Revisiting why DBDs can generate O_3 against the thermodynamic limit, *Int. J. Plasma Environ. Sci. Technol.*, Vol. 17, e02004, 2023.

[2] Weltmann K.-D., Kolb J. F., Holub M., Uhrlandt D., Šimek M., Ostrikov K., Hamaguchi S., Cvelbar U., Černák M., Locke B., Fridman A., Favia P., and Becker K., The future for plasma science and technology, *Plasma Process Polym.*, Vol. 16 (1), 1800118, 2019.

[3] Koinuma H., Ohkubo H., Hashimoto T., Inomata K., Shiraishi T., Miyanaga A., and Hayashi S., Development and application of a microbeam plasma generator, *Appl. Phys. Lett.* , Vol. 60 (7), pp. 816−817, 1992.

[4] Jeong J. Y., Babayan S. E., Tu V. J., Park J., Henins I., Hicks R. F., and Selwyn G. S., Etching materials with an atmospheric-pressure plasma jet, *Plasma Sources Sci. Technol.*, Vol. 7, pp. 282−285, 1998.

[5] Schutze A., Jeong J. Y., Babayan S. E., Jaeyoung P., Selwyn G. S., and Hicks R. F., The atmospheric-pressure plasma jet: a review and comparison to other plasma sources, *IEEE Trans.Plasma Science*, Vol. 26 (6), pp. 1685−1694, 1998.

[6] Laroussi M. and Lu X., Room-temperature atmospheric pressure plasma plume for biomedical applications, *Appl. Phys. Lett.*, Vol. 87 (11), 113902, 2005.

[7] Laroussi M., 1995–2005: A Decade of innovation in low temperature plasma and its applications, *Plasma*, Vol. 2 (3), pp. 360−368, 2019.

[8] Laroussi M., Low-temperature plasma jet for biomedical applications: A review, *IEEE Trans. Plasma Sci.*, Vol. 43 (3), pp. 703−712, 2015.

[9] Busco G., Robert E., Chettouh-Hammas N., Pouvesle J.-M., and Grillon C., The emerging potential of cold atmospheric plasma in skin biology, *Free Radic. Biol. Med.*, Vol. 161, pp. 290−304, 2020.

[10] Ishikawa K., Takeda K., Yoshimura S., Kondo T., Tanaka H., Toyokuni S., Nakamura K., Kajiyama H., Mizuno M., and Hori M., Generation and measurement of low-temperature plasma for cancer therapy: A historical review, *Free Radic Res*, Vol. 57 (3), pp. 239−270, 2023.

[11] Lu X. and Laroussi M., Dynamics of an atmospheric pressure plasma plume generated by submicrosecond voltage pulses, *J. Appl. Phys.*, Vol. 100 (6), 063302, 2006.

[12] Laroussi M. and Akan T., Arc-free atmospheric pressure cold plasma jets: A Review, *Plasma Process Polym.*, Vol. 4 (9), pp. 777−788, 2007.

[13] Winter J., Brandenburg R., and Weltmann K. D., Atmospheric pressure plasma jets: an overview of devices and new directions, *Plasma Sources Sci. Technol.*, Vol. 24 (6), 064001, 2015.

[14] Reuter S., von Woedtke T., and Weltmann K.-D., The kINPen—a review on physics and chemistry of the atmospheric pressure plasma jet and its applications, *J. Phys. D: Appl. Phys.*, Vol. 51 (23), 233001, 2018.

[15] Surowsky B., Schlüter O., and Knorr D., Interactions of non-thermal atmospheric pressure plasma with solid and liquid food systems: A review, *Food Eng. Rev.*, Vol. 7 (2), pp. 82−108, 2014.

[16] Penkov O. V., Khadem M., Lim W.-S., and Kim D.-E., A review of recent applications of atmospheric pressure plasma jets for materials processing, *J Coat Technol Res.*, Vol. 12 (2), pp. 225−235, 2015.

[17] Corbella C., Portal S., and Keidar M., Flexible cold atmospheric plasma jet sources, *Plasma*, Vol. 6 (1), pp. 72−88, 2023.
[18] Alqutaibi A. Y., Aljohani A., Alduri A., Masoudi A., Alsaedi A. M., Al-Sharani H. M., Farghal A. E., Alnazzawi A. A., Aboalrejal A. N., Mohamed A.-A. H., and Zafar M. S., The Effectiveness of cold atmospheric plasma (CAP) on bacterial reduction in dental implants: A systematic review, *Biomolecules*, Vol. 13 (10), 1528, 2023.
[19] Cao Z., Walsh J. L., and Kong M. G., Atmospheric plasma jet array in parallel electric and gas flow fields for three-dimensional surface treatment, *Appl. Phys. Lett.* , Vol. 94 (2), 021501, 2009.
[20] Kim S. J., Chung T. H., Joh H. M., Cha J., Eom I. S., and Lee H., Characteristics of multiple plasma plumes and formation of bullets in an atmospheric- pressure plasma jet array, *IEEE Trans. Plasma Sci.*, Vol. 43 (3), pp. 753−759, 2015.
[21] Hasnain Qaisrani M., Li C., Xuekai P., Khalid M., Yubin X., and Xinpei L., Patterns of plasma jet arrays in the gas flow field of non-thermal atmospheric pressure plasma jets, *Phys. Plasmas*, Vol. 26 (1), 013505, 2019.
[22] Zhang B., Fang Z., Liu F., Zhou R., and Zhou R., Comparison of characteristics and downstream uniformity of linear-field and cross-field atmospheric pressure plasma jet array in He, *Phys. Plasmas*, Vol. 25 (6), 063506, 2018.
[23] Babaeva N. Y. and Kushner M. J., Interaction of multiple atmospheric-pressure micro-plasma jets in small arrays: He/O_2 into humid air, *Plasma Sources Sci. Technol.*, Vol. 23 (1), 015007, 2014.
[24] Wang S., Zhang J., Li G., and Wang D., Cold large-diameter plasma jet near atmospheric pressure produced via a triple electrode configuration, *Vacuum*, Vol. 101, pp. 317−320, 2014.
[25] O'Neill F. T., Twomey B., Law V. J., Milosavljevic V., Kong M. G., Anghel S. D., and Dowling D. P., Generation of active species in a large atmospheric-pressure plasma jet, *IEEE Trans. Plasma Sci.*, Vol. 40 (11), pp. 2994−3002, 2012.
[26] Abdelaziz A. A.., Kim H.-H., and Teramoto Y., Towards launching a stable wide plasma jet from a single tube: II. Scaling parameters from the tube geometry and electrical characteristics *J. Phys. D: Appl. Phys.*, Vol. 54 (39), 395204, 2021.
[27] Abdelaziz A. A., Kim H.-H., Teramoto Y., and Takeuchi N., Towards launching a stable wide plasma jet from a single tube: I. The importance of controlling the gas dynamics. , *J. Phys. D: Appl. Phys.*, Vol. 54 (39), 395203, 2021.
[28] Abdelaziz A. A., Teramoto Y., and Kim H.-H., Unveiling the formation and control of unique swirling discharge pattern in helium plasma candle device, *J. Phys. D: Appl. Phys.*, Vol. 55 (6), 065201, 2021.
[29] Kim H.-H., Takeuchi N., Teramoto Y., Ogata A., and Abdelaziz A. A., Plasma candle: A new type of scaled-up plasma jet device, *Int. J. Plasma Environ. Sci. Technol.*, Vol. 14 (1), e01004, 2020.
[30] Abdelaziz A. A. and Kim H.-H., Distinctive patterns and characteristics of neon jet launched from plasma candle device, *Plasma Process. Polym.*, Vol. 18 (4), 2000190, 2021.
[31] Sarani A., Nikiforov A. Y., and Leys C., Atmospheric pressure plasma jet in Ar and Ar/H_2O mixtures: Optical emission spectroscopy and temperature measurements, *Phys. Plasmas*, Vol. 17, 063504, 2010.
[32] Lu X., Naidis G. V., Laroussi M., and Ostrikov K., Guided ionization waves: Theory and experiments, *Phys. Rep.*, Vol. 540 (3), pp. 123−166, 2014.
[33] Jõgi I., Talviste R., Raud J., Piip K., and Paris P., The influence of the tube diameter on the properties of an atmospheric pressure He micro-plasma jet, *J. Phys. D: Appl. Phys.*, Vol. 47 (41), 415202, 2014.
[34] Talviste R., Jõgi I., Raud J., and Paris P., The effect of dielectric tube diameter on the propagation velocity of ionization waves in a He atmospheric-pressure micro-plasma jet, *J. Phys. D: Appl. Phys.*, Vol. 49 (19), 195201, 2016.
[35] Wu S., Lu X., Yue Y., Dong X., and Pei X., Effects of the tube diameter on the propagation of helium plasma plume via electric field measurement, *Phys. Plasmas*, Vol. 23 (10), 103506, 2016.
[36] Wang L., Zheng Y., and Jia S., Numerical study of the interaction of a helium atmospheric pressure plasma jet with a dielectric material, *Phys. Plasmas*, Vol. 23 (10), 103504, 2016.
[37] Karakas E., Koklu M., and Laroussi M., Correlation between helium mole fraction and plasma bullet propagation in low temperature plasma jets, *J. Phys. D: Appl. Phys.*, Vol. 43 (15), 155202, 2010.
[38] Xiong Q., Lu X., Ostrikov K., Xiong Z., Xian Y., Zhou F., Zou C., Hu J., Gong W., and Jiang Z., Length control of He atmospheric plasma jet plumes: Effects of discharge parameters and ambient air, *Phys. Plasmas*, Vol. 16 (4), 043505, 2009.
[39] Joh H. M., Kang H. R., Chung T. H., and Kim S. J., Electrical and optical characterization of atmospheric-pressure helium plasma jets generated with a pin electrode: effects of the electrode material, ground ring electrode, and nozzle shape, *IEEE Trans. Plasma Sci.*, Vol. 42 (12), pp. 3656−3667, 2014.